Model Investigations of Unstiffened and Stiffened Circular Shells

Test techniques used in evaluation of the effect of internal pressure on stability of shells used in modern aircraft and missiles are described; also, conclusions derived from the results are presented and discussed

by L. A. Harris, H. S. Suer and W. T. Skene

ABSTRACT— In 1951, an extensive review of the literature indicated that only a limited amount of test data was available to evaluate the effect of internal pressure on the stability of unstiffened and stiffened circular cylindrical shells. In addition, data on the postbuckling strength of stiffened cylinders were also limited. Because of the importance of the cylindrical shell in missile construction, an extensive investigation was initiated to provide such data. The present paper includes a description of the test techniques used in these investigations and some conclusions derived from the results.

Nomenclature

- A = total sheet area ($2\pi rt$).
- A_s = area of all stringers.
- E = modulus of elasticity.
- G = shear modulus.
- L = length of cylinder.
- R_p = ratio of internal pressure to critical external pressure (p/p_0).
- R_τ = ratio of critical shear stress with internal pressure to critical shear stress under torsion alone (τ/τ_0).
- T_{cr} = panel buckling torque.
- a = spacing of ring stiffeners.
- b = spacing of stringers.
- p = internal pressure.
- p_0 = critical external pressure (considered negative).
- r = radius of cylinder.
- t = thickness of cylinder.
- t_s = thickness of stringer material.
- θ = angle of buckles with longitudinal axis of cylinder.
- μ = Poisson's ratio.
- σ_1 = longitudinal sheet stress.
- σ_a = average axial stress (total end pressure load divided by area of skin and stringers).
- σ_s = stringer stress.
- τ = critical shear stress with internal pressure.
- τ_0 = critical shear stress under torsion alone.

Introduction

In modern aircraft and missiles, extensive use is made of pressurized, unstiffened and stiffened circular cylindrical shell structures. Even though these shells may not be pressurized for structural purposes, systems requirements often dictate the use of internal pressure. Because internal pressure materially increases the buckling stress of circular shells, a considerable weight saving can be achieved by taking advantage of this increase in buckling strength.

When the experimental investigation described herein was initiated in 1951, test data on the effect of internal pressure on the stability of circular cylindrical shells were limited. The available data for both unstiffened and stiffened shells did not encompass the parameter ranges likely to be encountered in modern aircraft and missile structure. It was apparent that empirical data were required to obtain reliable design information. As a consequence, an extensive investigation of model circular cylindrical shells was initiated to provide some of these data.

A test jig was developed to apply axial compression, bending, torsion and external pressure, either singly or in combination. The jig also allowed the application of internal pressure. By proper dimensional scaling, model cylinders could be selected that were parametrically equivalent to full-scale structures. This equipment permitted the use of low-cost models in lieu of full-scale structure.

Initially, the unstiffened shells were fabricated from fiberglass or Mylar sheet. However, shortly after the beginning of the program, foil-gage aluminum and stainless steel became available and these materials were used in the majority of tests. Many of the specimens were fabricated with a single longitudinal, adhesive-bonded lap joint. Some of the later unstiffened cylinders were seam welded, which proved to be a satisfactory technique. Adhesive bonding was also used in the fabrication of the ring and stringer reinforced test shells. Unfortunately, the stiffened cylinders could not be used to study the ultimate strength of the shell because pre-

L. A. Harris is Supervisor, Structural Mechanics, Space and Information Systems Division, North American Aviation, Inc.; H. S. Suer is Section Head, Ground Systems Dynamics, Space Technology Laboratories, Inc. (formerly Senior Structures Engineer, S&ID); and W. T. Skene is Manager, Applied Research, Space and Information Systems Division, North American Aviation, Inc.

Paper was presented at 1959 SESA Spring Meeting held in Washington, D. C., on May 20–22.

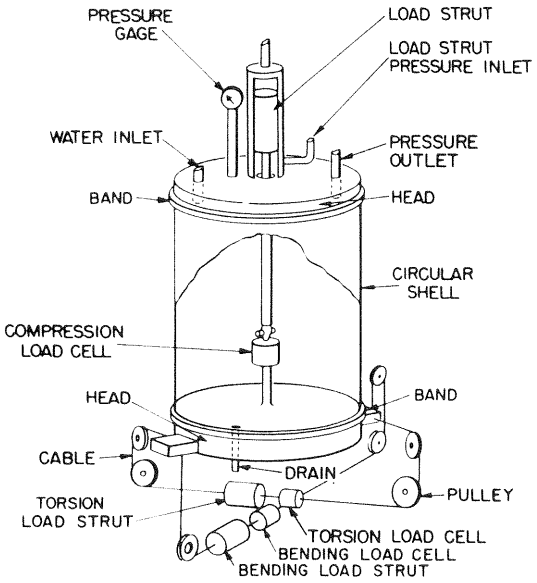

Fig. 1—Test-jig schematic

mature failure was induced in the bond between the skin and the stringers.

The present paper includes a description of the test techniques used in these investigations and presents the results of some of the tests.

Unstiffened Cylinders

Test Specimens

At the initiation of the investigation, metal foil was not available in large sizes and, as a result, the first specimens were fabricated from fiberglass or mylar with a single longitudinal, adhesive-bonded lap joint. Although the fabrication and testing of these specimens were satisfactory, it was found that the mechanical properties of these materials varied from specimen to specimen and consistent results were difficult to obtain. Early in the program, foil-gage 2S-H-18 aluminum alloy and 18-8 half-hard stainless steel became available in rolls up to 36 in. wide, and these materials were used to fabricate the specimens for the remaining tests.

Over 200 test cylinders were fabricated from stainless steel and aluminum-alloy foils. The cylinders were fabricated with a $^3/_8$-in. wide longitudinal lap joint bonded with Epon VI adhesive which was cured under pressure at 200° F. Use of adhesive bonding had the advantage that residual stresses were reduced. The bonded joint did not appear to interfere with the buckle pattern in any of the specimens. Some of the later test specimens were fabricated by seam welding, which proved to be a faster and simpler technique. Although some wrinkling occurred at the seam of the welded cylinders, no appreciable difference could be noted between the buckling stresses of the bonded and of the welded cylinders.

The test cylinders were fabricated from 0.005-inch-thick aluminum foil and 0.0032-, 0.004- and 0.0087-in. stainless-steel foil. These sheet thicknesses were the averages of a number of micrometer measurements, and the maximum variation in thickness from the mean was less than 10%. The cylinders were tested with unsupported lengths of 9.5 and 22.5 in. The length of the cylinder was perpendicular to the direction of rolling of the sheet material. Sample specimens of the foil were regularly tested to determine the modulus of elasticity and the compressive yield strength of the aluminum and steel. The modulus of elasticity used in evaluating the test data was 10.5×10^6 and 27.0×10^6 psi, respectively, for the aluminum and stainless-steel foils.

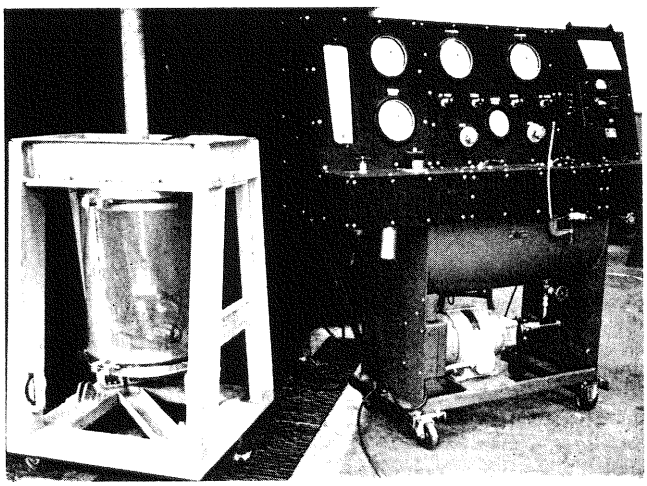

Fig. 2—Test apparatus with Mylar cylinder in position for test

Fig. 3—Ripples in pressurized torsion specimen prior to buckling

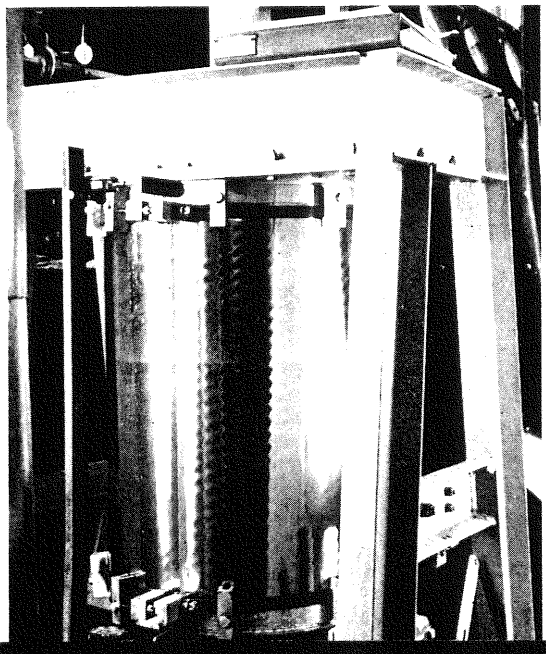

Test Apparatus and Procedures

A jig was developed to test circular cylinders 18½ in. in diameter and of variable lengths. A schematic drawing of the jig is shown in Fig. 1, and a mylar cylinder is shown in position for testing in Fig. 2.

The test cylinders snugly fitted the lower and upper 3-in. aluminum heads of the test jig. The cylinders were pressed carefully onto these heads. The cylinder was placed on the lower head, and the internal strut and load cell were connected. The lower head was raised slowly by hydraulic pressure and, at the same time, the cylinder was guided on to the upper head of the jig. The cylinder was stabilized by a small internal pressure to prevent damage as it slipped over the upper head. As the lower head continued to rise, the position of the cylinder on the heads was carefully measured and the lower head was guided to keep the cylinder square on the heads.

Each cylinder was firmly clamped to the heads with rubber-lined steel bands which were tightened with bolts to a predetermined torque. To hold the cylinder more tightly to the heads, eight lugs were screwed against each band. The bands prevented slippage and leakage between the heads and the cylinder.

Compressive, bending and torsion loads were applied to the cylinder with hydraulic struts and were measured with Baldwin type U-1 SR-4 strain indicators. The axial strut and the load cell for compression are visible through the transparent mylar cylinder in Fig. 2. The bending moment or torque was applied to the bottom head by two cables which were activated by a hydraulic strut. The pulley-cable loading system for applying these loads is shown schematically in Fig. 1. Heavy-duty ball-bearing aircraft pulleys and ¹⁄₄-in. steel cables were used to apply these loads. A check test indicated that the friction in the pulley system was negligible, which assured equal loads in both cables. Internal pressurization was pneumatically applied and was varied from 0 to about 24 psi. External pressure was applied by partially evacuating the cylinders.

The control console shown in Fig. 2 was used to regulate the strut pressures. The loads were measured by SR-4 load cells. Internal or vacuum pressure was generally measured by a 5-ft mercury manometer reading to 0.1 in. A Wallace-Tiernan dial manometer with a least reading of 0.05 in. of water was used to read low pressures.

Before applying any other load, a compressive force equal to the dead weight of the lower head of the test jig was applied to the specimen. In the bending and torsion tests, an additional compressive load could also be applied to the lower head to balance the longitudinal tension force applied by the internal pressure. For combined loadings, the order of application of loads had no effect on the magnitude of the critical stresses.

When the internal pressure exceeded 2 psi, the test cylinders were partially filled with water for safety purposes and the average internal pressure reported. The dead weight of the water was balanced by the central load strut.

The buckling loads of the test specimens were determined visually. For most specimens, a visual determination of the buckling load was relatively simple because the buckles often snapped in position. Occasionally buckles appeared to grow out of relatively large initial irregularities. Incipient buckling of a pressurized cylinder was often indicated by the formation of circumferential ripples. Although initially very shallow, these ripples could be seen easily in the reflected surface of the cylinder, as shown in Fig. 3 for torsion. The load at which buckles with well-defined longitudinal and transverse wave lengths

Fig. 4—Typical buckle pattern for unpressurized cylinder in compression

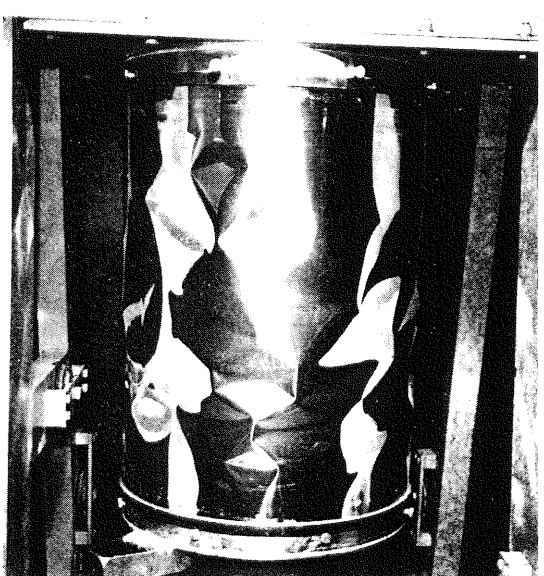

Fig. 5—Typical buckle pattern for pressurized cylinder in compression

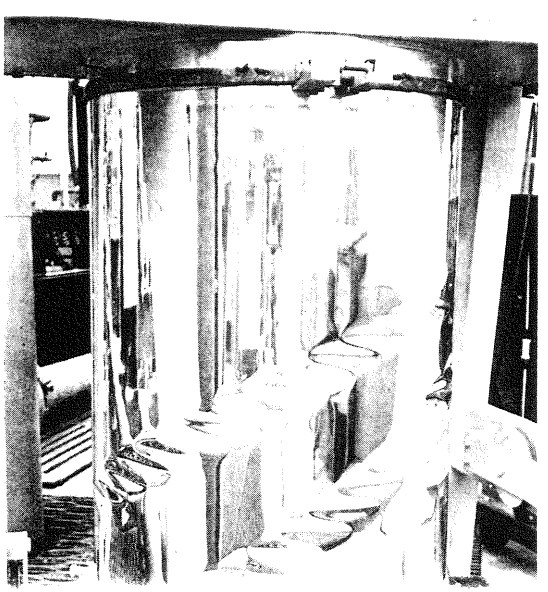

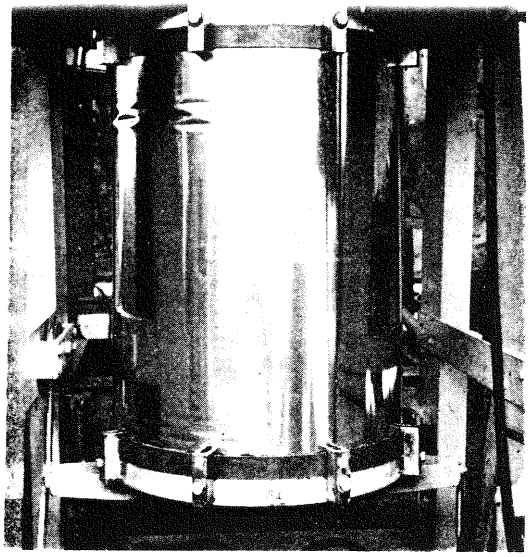

Fig. 6—Typical buckle pattern for pressurized cylinder in bending

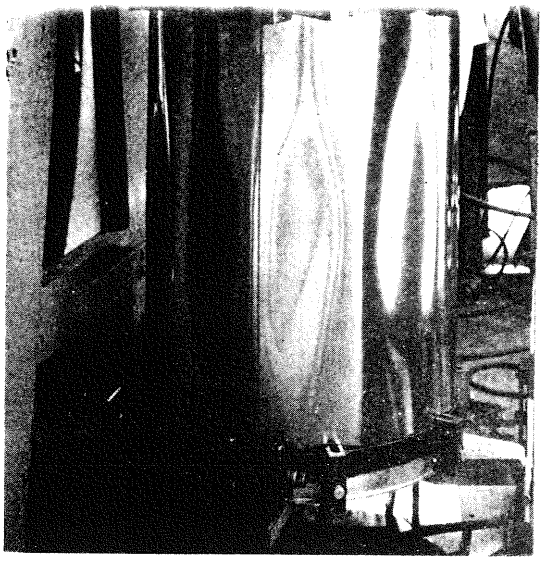

Fig. 7—Typical buckle pattern for hydrostatic pressure

formed was always within 10% of the initial rippling. Just prior to buckling, the ripples often extended over the entire length of the cylinder.

The final buckle pattern extended only over a portion of the cylinder. In the case of pressurized cylinders, generally only one or two series of buckles occurred. The buckles appeared to be elastic and visually disappeared upon removal of the load. Some of the cylinders were retested with equal or larger internal pressure. Slightly lower values of critical stress were often obtained with equal pressure, indicating that some permanent distortion of the shell had occurred during the previous test.

Test Results

For the unstiffened cylinders, five loading conditions have thus far been studied: pressurized cylinders in compression, bending and combined compression and torsion; combined external pressure and torsion; and pressurized cylinders in torsion. The analysis of the data and recommended design curves for the first four of the loadings have been reported in previous papers.[1-4] Typical buckle patterns for these loading conditions are shown in Figs. 4 through 10. The results of the tests of pressurized cylinders in torsion are presented below.

The effect of internal pressure on the torsional buckling stress has been considered in two previous papers. Crate, Batdorf and Baab[5] developed a semi-empirical interaction formula, $R_p + R_s^2 = 1$, for combined pressure and torsion based on a limited series of tests. Hopkins and Brown[6] derived a small deflection theoretical analysis by modifying Donnell's original analysis for unpressurized cylinders. Their theoretical calculations generally agreed well with the experimental results of Reference 5 and sub-

TABLE 1—RESULTS OF TESTS OF UNSTIFFENED CYLINDERS IN TORSION
18-8 half-hard stainless steel, $E = 27 \times 10^6$ psi, r = 8.75 in., L = 22.5 in.

Specimen No.	r/t	p, psi	τ, psi	θ, deg	Specimen No.	r/t	p, psi	τ, psi	θ, deg
				Unpressurized					
112-1	1006	0	2162	..	95-1	2734	0	569	..
114-1	1006	0	2256	18	223-1	2734	0	250	10
94-1	2734	0	487	..	..	..	..	..	..
				Pressurized					
204-1	1006	4.4	7407	30	109-1	2734	2.4	4688	45
205-1	1006	4.4	7168	..	105-1	2734	4.4	6173	..
203-1	1006	8.4	9582	45	106-1	2734	8.4	10559	..
206-1	1006	8.4	9295	..	266	2734	8.4	9542	70
202-1	1006	16.4	14600	45	267	2734	8.4	9502	70
207-1	1006	16.4	12903	45	268	2734	8.4	9542	65
217-1	1006	20.4	14409	50	107-1	2734	16.4	14620	..
218-1	1006	20.4	14791	55					

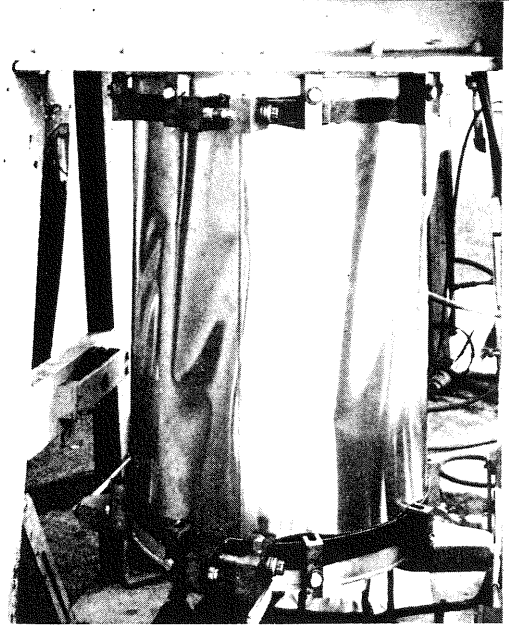

Fig. 8—Typical buckle pattern for combined torsion and external pressure

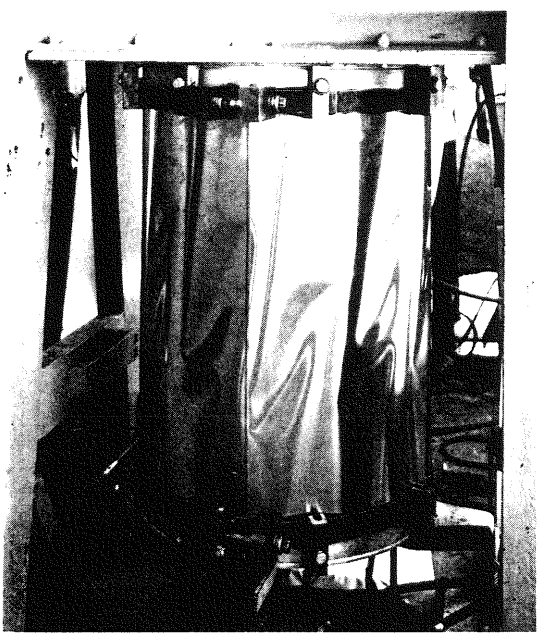

Fig. 9—Typical buckle pattern for unpressurized cylinder in torsion

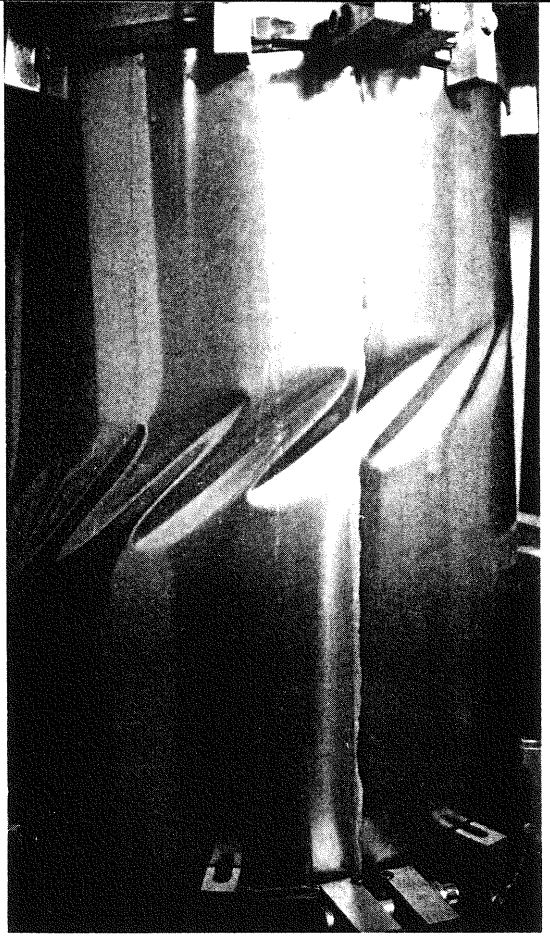

Fig. 10—Typical buckle pattern for pressurized cylinder in torsion

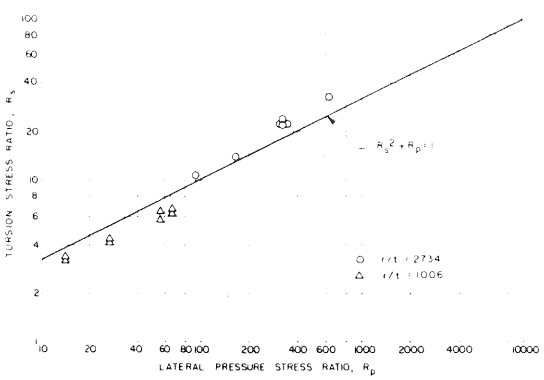

Fig. 11—Interaction curve for cylinders in torsion with lateral internal pressure

stantiated the semi-empirical interaction curve. The present investigation was made to extend the test data to the range of internal pressures and radius to thickness ratios of current interest in missile and aircraft design.

A total of 5 unpressurized and 15 pressurized model circular cylinders were tested in torsion. For the internally pressurized specimens, the longitudinal tensile stresses induced by pressure were balanced by a compressive load. The geometry of the cylinders and the test data are given in Table 1. A photograph of a typical buckle pattern for an unpressurized cylinder is shown in Fig. 9 and for a pressurized cylinder in Fig. 10. As expected, the angle which the buckles made with the axis of the cylinder increased as the ratio of the internal pressure to the torque increased (refer to Table 1).

In Fig. 11, the test data are compared to the interaction curve of Reference 5. In calculating the val-

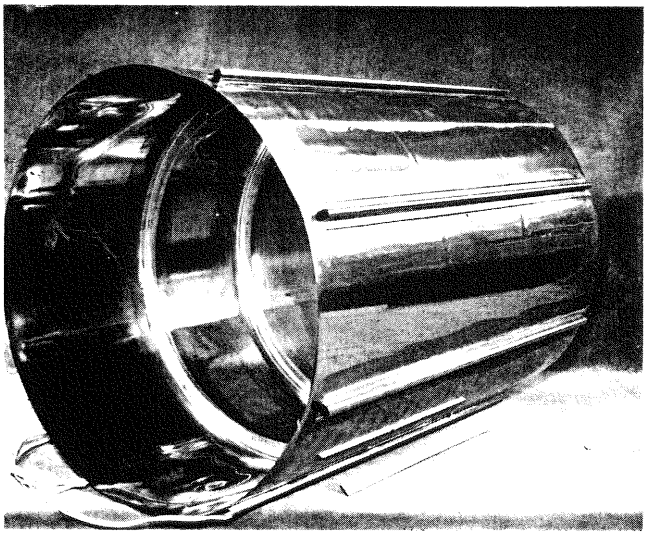

Fig. 12—Model stiffened cylinder

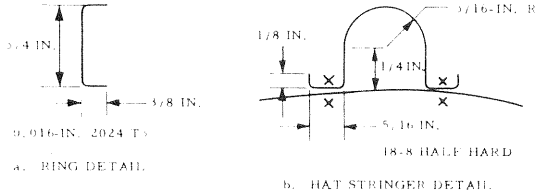

Fig. 13—Stiffener details and strain-gage locations

ues of R_s, the buckling stress for torsion alone has been defined as the average of the experimental values. In calculating the values of R_p, the buckling stress for external lateral pressure alone has been calculated from Reference 7. It may be seen in Fig. 11 that the interaction curve adequately describes the behavior of circular cylinders in torsion with internal lateral pressure. Based on the present data, the interaction curve of Fig. 11 is recommended for design within the range of parameters investigated.

It should be noted that the experimental data of Fig. 11 are for cylinders under lateral pressure only and, therefore, the data indicate the direct benefit of

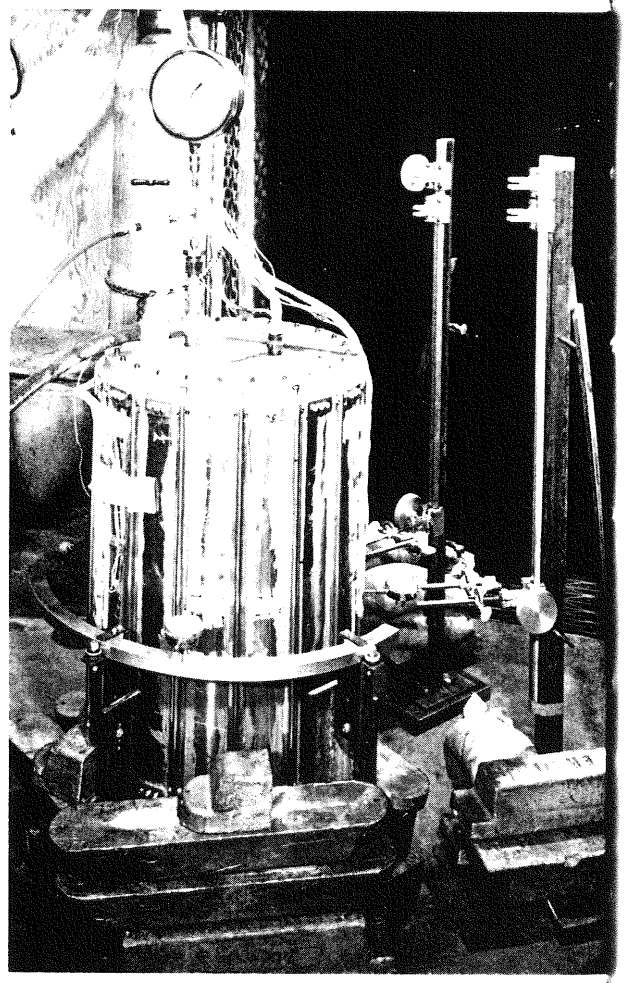

Fig. 14—Test setup for internal pressurization of stiffened cylinders

internal lateral pressure on the torsional buckling stress. If, in addition, the cylinder is axially pretensioned to a stress of $pr/2t$ by the internal pressure on the cylinder heads, an additional benefit would result. It can easily be shown by a Mohr's circle construction that a torsional stress of $0.707\ pr/t$ is required before compression is induced in the skin of a hydrostatically pressurized cylinder. At low values of pr/t, the benefit of the axial tension is relatively small but, at large values of pr/t, the effect of the axial stress induced by internal pressure would be expected to predominate.

Stiffened Cylinders

Whereas unstiffened cylinders can be scaled by reducing the thickness of the skin, radius and length, a proper scaling of stiffened cylinders requires also a scaling of rings, stringers and attachments. This has been difficult to accomplish inexpensively. Scaling of the attachments is especially difficult.

TABLE 2—RESULTS OF TESTS OF STIFFENED CYLINDERS

Specimen No.	t, in.	t_a, in.	p, psi	a, in.	b, in.	T_{cr}, kip-in.	θ, deg	G(psi) Before T_{cr}	G(psi) After T_{cr}
1	0.0087	0.0087	40.4	7.08	2.75	..	..	..	..
2	0.0087	0.0087	40.4	7.08	2.75	..	..	..	..
3S	0.0032	0.0032	3.7	7.08	6	10	45	11.0×10^6	[b]
4S	0.0032	0.0032	0	7.08	6	[b]	20	[b]	1.0×10^6
			1			3/5.5[a]	35	10.9×10^6	1.0×10^6
			2			6/9	40	8.6×10^6	1.0×10^6
5S	0.0032	0.0032	3.7	7.08	6	10/15	40	9.47×10^6	1.0×10^6
6S	0.0087	0.0087	0	14.7	6	7/7	15	[b]	1.2×10^6
7S	0.0087	0.0087	8.4	14.7	6	50[b]	40	9.5×10^6	[b]
8S	0.0032	0.0087	0	14.7	6	[b]	15	[b]	1.6×10^6
9S	0.0032	0.0087	3.4	14.7	6	10/13	35	8.7×10^6	1.8×10^6
10S	0.0087	0.0087	4.3	14.7	6	32/38	35	11.8×10^6	0.9×10^6
11S	0.0087	0.0087	4.3	14.7	6	31/39	30	10.3×10^6	0.8×10^6
								10.0×10^6 (average)	1.1×10^6 (average)

[a] The lower torque is the initial buckling and the high torque is obtained from the interaction of the load deflection curves in the unbuckled and the buckled states.
[b] Insufficient data.

The present tests were initiated to investigate the feasibility of fabricating small-scale models economically by adhesive-bonding techniques. In particular, the use of adhesive bonding considerably simplifies the attachment of the stiffeners to the shell.

Two problems were chosen for study in this pilot series: (1) the stress distribution in the stringers and skins of pressurized stiffened cylinders and (2) the tension-field behavior of unpressurized and pressurized stiffened cylinders. The data obtained were the stress distribution due to internal pressure and/or torsion, the panel buckling torques, and the effect of internal pressure on the torque-rotation relationship. It was intended to obtain data on the ultimate strength and mode of failure but premature failures of the adhesive bond occurred. Described herein are the fabrication of the model cylinders, the test equipment and procedures, and the test results.

Test Specimens

A photograph of a typical test specimen is shown in Fig. 12. The cylinders were fabricated from 0.0032- and 0.0087-in. thick, half-hard 18-8 stainless-steel foil. They had a length of 22½ in., a radius of 8.75 in. and r/t ratios of approximately 1000 and 2730. The stringers were formed from the same material to the shape shown in Fig. 13. The ring stiffeners were formed from 2024-T3 aluminum alloy to the cross section shown in Fig. 13. The location of the internal rings and the number of external stringers were varied during the test program. Table 2 summarizes the important dimensions of the cylinders.

The fabrication sequence for the shells was as follows: (1) the longitudinal seam of the shell was

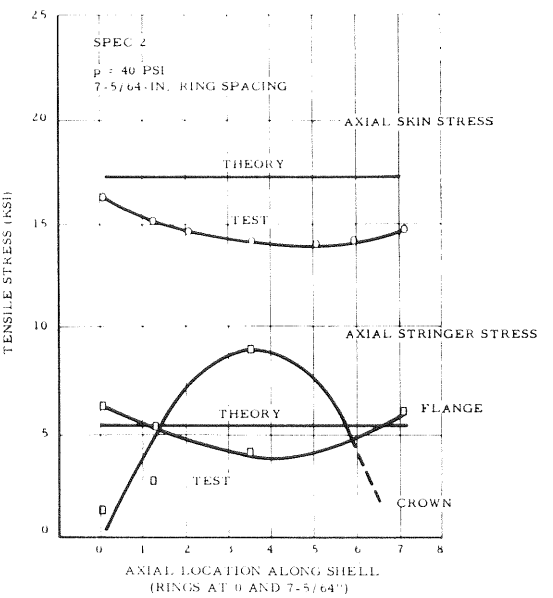

Fig. 15—Stress distribution from internal pressure

bonded, (2) the hat-section stringers were bonded to the outside surface of the shell and (3) the aluminum rings, which were split to allow a reduction in diameter for insertion inside the cylinder, were then bonded in place. Rings, stringers and cylinders were bonded under temperature and pressure with Epon VI adhesive.

Test Apparatus and Procedures

For the tests to investigate the stress distribution under pressure alone, both the sheet and the stringers were bolted to 1-in.-thick heads, as shown in Fig. 14.

Doubler strips and fittings were used at the ends to provide sufficient contact area. The test jig used for the torsion tests of stiffened cylinders was the same as that described for unstiffened shells, with clamps to bolt the stringer ends to the top and bottom heads. The clamps were required to transfer the high-tension-field stringer loads to the heads.

Strain rosettes were placed back-to-back on the skin panels, and six axial gages were mounted across sections of the stringer between rings. A typical strain-gage layout is shown in Fig. 13. One of the strain gages was located on the inside of the hat section and becomes inaccessible during subsequent fabrication of the shell. As a consequence, this gage was mounted and the wires were attached and insulated before assembly of the test specimen. For most specimens, strain gages were located at five sections along the stringers between rings.

For the torsion specimens, dial indicators were used to measure the rotation of the movable lower head of the jig with respect to the upper fixed head. These measurements were used to establish the torque-rotation relationships.

Fig. 16—Buckle pattern for pressurized stiffened cylinders in torsion

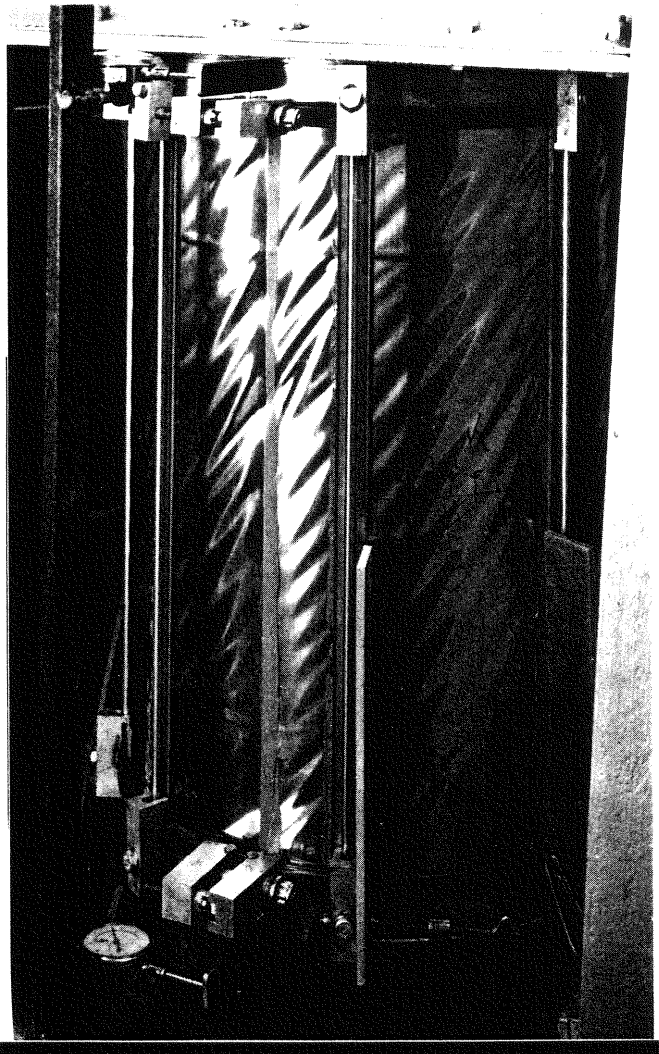

Test Results

STRESSES INDUCED BY INTERNAL PRESSURE—A comparison between theory and test is shown in Fig. 15 for a typical specimen. The data shown are the relationships between the axial sheet and stringer stresses as a function of the distance between rings. Crown and flange stresses are shown for the stringer. Internal pressure causes an outward bowing of the stringers between rings as indicated by the crown and flange stresses.

Theoretical predictions of the longitudinal sheet and average stringer stresses, neglecting stresses induced by compatibility of strains between stringers, rings and sheet, are shown in Fig. 15. The analysis[5] is based on equal axial deformations for the sheet and the stringers which gives

$$\sigma_1 = \sigma_a \left(1 + 2\frac{A_s}{A}\frac{\ell}{\ell}\right)$$
$$\sigma_2 = \sigma_a(1 - 2\mu)$$

Note that the average longitudinal sheet and stringer stresses are not equal. This inequality is a result of the Poisson's ratio effect which occurs in the sheet under biaxial tension but is absent in the longitudinally stressed stringers.

Good agreement was found between test and theory for the midspan average stringer stress, but the stresses adjacent to the rings are significantly different than predicted. The experimentally determined axial skin stress is a maximum of about 25% less than predicted.

TENSION-FIELD BEHAVIOR For this series of specimens, the torque was applied after the cylinder had been pressurized. A photograph of highly developed tension-field buckles in a typical specimen is shown in Fig. 16.

The torsional rigidity of the prebuckled and postbuckled cylinders was studied by measuring the rotation of the lower end of the cylinder with respect to the upper fixed end. Table 2 summarizes the data from the cylinders under torsion. Plots of the torque-rotation data for one configuration are shown in Fig. 17. It is significant to note that the torsional ridigities of both the unpressurized and the pressurized shell are approximately the same after, as well as before, panel buckling. The torque at which buckling occurs is increased, of course, as the internal pressure is increased (refer to Table 2). The shear modulus of the unbuckled shells averaged 10.0×10^6 psi for all the specimens, whereas the theoretical value, $G = E/2(1 + \mu)$, would be 10.5×10^6 psi. The shear rigidity calculated from the postbuckling portion of the curve averaged 1.1×10^6 psi and appeared to be the same as for the unpressurized shell at pressures up to 3.7 psi.

The stringer stress distribution caused by diagonal tension is shown in Fig. 18 for a cylinder with a 0.0032-in.-thick skin, 0.0087-in.-thick stringer material and an aspect ratio of about 2. The effect of torque on the stringer stress is negligible until sheet buckling occurs. Then, diagonal tension in the sheet significantly increases the stringer axial stresses and

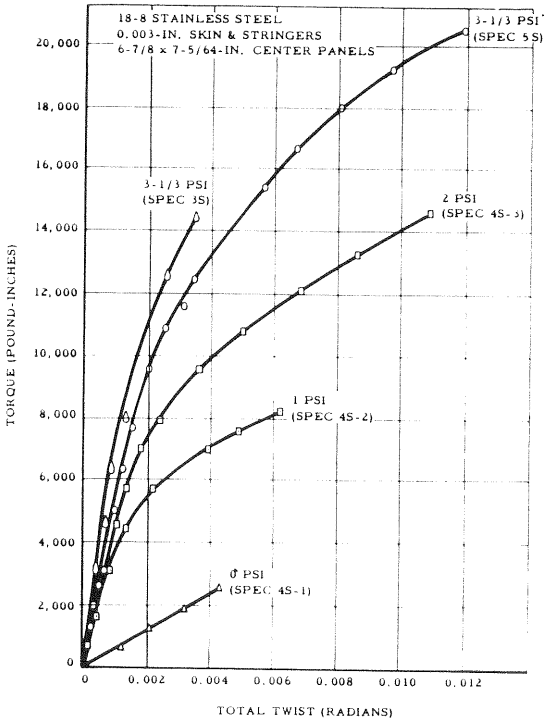

Fig. 17—Typical torque-rotation results for stiffened cylinders

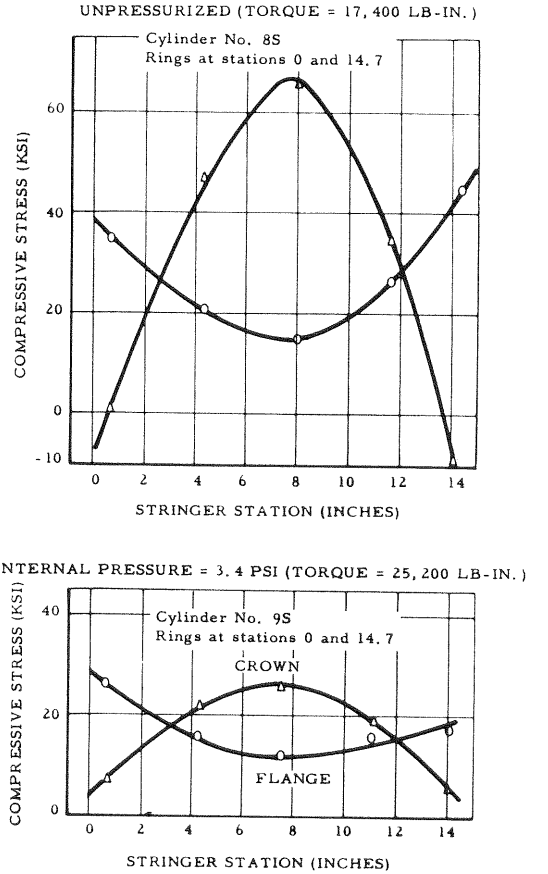

Fig. 18—Typical diagonal tension stringer stresses

applies an inward radial load which causes bending in the stringer. In Fig. 18 are shown graphs of stringer stresses induced in unpressurized and pressurized cylinders by tension-field action. Note that the distribution of the bending stress caused by torsion of the unpressurized cylinder is similar to that caused by internal pressure, but is of the opposite sign. As a consequence, the diagonal tension stringer axial and bending stresses are partially relieved by the internal pressure axial and bending stresses, as indicated in Fig. 15. This partial balancing of stresses may have important beneficial effects in those cases in which forced crippling of the compression side of the stringer precipitates ultimate failure of the stiffened shell.

It was intended that the test specimens should provide data on the ultimate strength as well as the stringer and skin stress distribution before and after buckling of the panels. However, most of the specimens failed prematurely either in the longitudinal seam or as a result of buckles forcing their way under the stringers and destroying the adhesive-bonded joint. Although difficulties of this kind were encountered, it is nevertheless believed that proper design of the test specimen and the use of the proper adhesive would make the specimens useful for studies of ultimate failures.

Acknowledgment

The authors gratefully acknowledge the assistance of the personnel of the Missile Division Laboratory.

References

1. *Harris, L. A., Suer, H. S., Skene, W. T., and Benjamin, R. J., "The Stability of Thin-Walled Unstiffened Circular Cylinders Under Axial Compression Including the Effects of Internal Pressure," Jnl. Aero. Sci., 24, No. 8, 587 596 (August 1957).*
2. *Suer, H. S., Harris, L. A., Skene, W. T., and Benjamin, R. J., "The Bending Stability of Thin-Walled Unstiffened Circular Cylinders Including the Effects of Internal Pressure," Ibid., 25, No. 5, 281 287 (May 1958).*
3. *Harris, L. A., Suer, H. S., and Skene, W. T., "The Effect of Internal Pressure on the Buckling Stress of Thin-Walled Cylinders Under Combined Axial Compression and Torsion," Ibid., 25, No. 2, 142 143 (February 1958).*
4. *Suer, H. S., and Harris, L. A., "The Stability of Thin-Walled Cylinders Under Combined Torsion and External Lateral or Hydrostatic Pressure," Jnl. Appl. Mech., 81, series E, No. 1, 138 140 (March 1959).*
5. *Crate, H., Batdorf, S. B., and Baab, G. W., "The Effect of Internal Pressure on the Buckling Stress of Thin-Walled Circular Cylinders Under Torsion," NACA L4k27, May 1944.*
6. *Hopkins, H. C., and Brown, E. H., "The Effect of Internal Pressure on the Initial Buckling of Thin-Walled Circular Cylinders Under Torsion," British Aeronautical Research Council, R&M No. 2423, January 1950.*
7. *Batdorf, S. B., "A Simplified Method of Elastic-Stability Analysis for Thin Cylindrical Shells," NACA Report 874, 1947.*
8. *Martin, V. I., and Smith, N. Y., "Relation Between Stringer Stress and Longitudinal Sheet Stress in a Reinforced Cylindrical Shell Under Internal Pressure," Aerophysics Laboratory Report PDM-8, North American Aviation, Inc., October 1950.*